

# Sparsity based Terahertz reflective off-axis digital holography

Min Wan<sup>1,2</sup>, Inbarasan Muniraj<sup>2</sup>, Ra'ed Malallah<sup>2,3</sup>, Liang Zhao<sup>2,4</sup>, James P Ryle<sup>2</sup>, Lu Rong<sup>1,5</sup>, John J Healy<sup>2</sup>, Dayong Wang<sup>1,5</sup>, John T Sheridan<sup>2\*</sup>.

<sup>1</sup>College of Applied Sciences, Beijing University of Technology, Beijing, 100124, China.

<sup>2</sup>School of Electrical and Electronic Engineering, University College Dublin, Belfield, Dublin 4, Ireland.

<sup>3</sup>Physics Department, Faculty of Science, University of Basrah, Garmat Ali, Basrah, Iraq.

<sup>4</sup>Insight of Data analytics, University College Dublin, Belfield, Dublin 4, Ireland.

<sup>5</sup>Beijing Engineering Research Centre of Precision Measurement Technology and Instrument, Beijing University of Technology, Beijing, 100124, China.

[\\*john.sheridan@ucd.ie](mailto:john.sheridan@ucd.ie)

## ABSTRACT

Terahertz radiation lies between the microwave and infrared regions in the electromagnetic spectrum. Emitted frequencies range from 0.1 to 10 THz with corresponding wavelengths ranging from 30  $\mu\text{m}$  to 3 mm. In this paper, a continuous-wave Terahertz off-axis digital holographic system is described. A Gaussian fitting method and image normalisation techniques were employed on the recorded hologram to improve the image resolution. A synthesised contrast enhanced hologram is then digitally constructed. Numerical reconstruction is achieved using the angular spectrum method of the filtered off-axis hologram. A sparsity based compression technique is introduced before numerical data reconstruction in order to reduce the dataset required for hologram reconstruction. Results prove that a tiny amount of sparse dataset is sufficient in order to reconstruct the hologram with good image quality.

**Keywords:** Terahertz imaging; Digital holography; Sparsity.

## 1. INTRODUCTION

The terahertz region (0.1 GHz–10 THz) is a significant part of the electromagnetic radiation spectrum, which lies between the microwave and infrared regions. The use of coherent THz radiation for imaging is gaining attention as it's more a powerful tool for material science and mechanical engineering [1]. Over the past two decades, research on Terahertz (THz) technology has shown potential in practical applications (biomedical imaging) due to the ability of THz radiation to penetrate various non-conducting materials that are opaque for visible light [2, 3]. The combination terahertz digital holography takes the advantages of both the terahertz radiation and the digital holography, thus making up the defects of conventional holographic systems and in fact broadens the applications of holography [4-7]. It is known that due to various applications such as fast processing, compatibility and computer generated holograms (CGHs) to name a few, the use of photoelectric sensors (CCD, CMOS) in recording interferograms (i.e., digital holography) and numerical reconstruction have received wide attention [8-12].

Digital holography (DH) is a discrete whole-field imaging technique where both the intensity and phase components of a wave-field are captured using the holographic principle [13]. Numerical reconstruction of the digitally recorded intensity hologram enables access to the intensity and phase of the object field [12]. One common problem in recording and processing digital holograms is voluminous dataset, i.e., a huge amount of information have to recorded and processed which makes the process extremely (computationally) difficult. For this reason, methods such as data compression, compressive sensing have been proposed and implemented [14-18]. In this paper, for the first time, in order

to reduce the complexity in processing the digitally recorded holograms, we propose to use a Sparsity-based hologram compression. The method sparsity refers to randomly selecting some pixel information by discarding most of the data, however, reconstruction can be achieved with minimal loss [19, 20]. This approach will certainly reduce the dataset required for reconstruction (with reduced MSE value) and facilitates more efficient storage and data transmissions.

The rest of our paper is organised as follows: In Section 2, we briefly discuss the Terahertz based off-axis holographic imaging system. Section 3 describes our experimental setup. Results are given in Section 4 and conclusion is presented in Section 5.

## 2. OFF-AXIS DIGITAL HOLOGRAPHY

Off-axis digital holographic method refers to recording holograms using digital sensors and employing numerical methods for reconstruction, enabling thus the applications of advanced holography. In principle, the laser beam is divided by a beam splitter, in which a part of beam is reflected or scattered by the object (known object arm) and interferes with the non-scattered beam (i.e., reference arm). The interference pattern (i.e., hologram) is recorded using digital cameras [8]. Assuming that the object and recording plane coordinates are  $x_o$ - $y_o$  and  $x$ - $y$  respectively, the object complex distribution on the object plane can be expressed as,

$$O(x_o, y_o) = o(x_o, y_o) \exp[j\phi(x_o, y_o)] \quad (1)$$

where the  $o(x_o, y_o)$  and  $\phi(x_o, y_o)$  are the amplitude and phase distribution, respectively. The propagation of object wave towards the recording plane is calculated using the angular spectrum propagation integral, as follows [21]:

$$O_d(x, y) = \mathfrak{F}^{-1} \left\{ \mathfrak{F}[O(x, y)] \exp \left[ jkd \sqrt{1 - (\lambda f_x)^2 - (\lambda f_y)^2} \right] \right\} \quad (2)$$

where  $\lambda$  is the wavelength,  $k=2\pi/\lambda$  is the wave number and  $d$  is the reconstruction distance.  $\mathfrak{F}$  and  $\mathfrak{F}^{-1}$  denotes the Fourier transform and inverse Fourier transform respectively. The exponential function,  $\exp \left[ jkd \sqrt{1 - (\lambda f_x)^2 - (\lambda f_y)^2} \right]$  represents the transfer function of the wave propagation through free space [22, 23]. The functions  $f_x = x/(N_x \Delta x)$  and  $f_y = y/(N_y \Delta y)$  are the spatial frequencies of horizontal and vertical directions in the spatial frequency domain.  $N_x$  and  $N_y$  are the number of pixels,  $\Delta x$  and  $\Delta y$  are the pixel size of the detector. Assuming the complex amplitude distribution of the reference wave  $R_d(x, y)$ , the off-axis digital hologram can be expressed as [18],

$$H(x, y) = |O_d(x, y) + R_d(x, y)|^2 = |O_d|^2 + |R_d|^2 + O_d R_d^* + O_d^* R_d \quad (3)$$

where the first two terms on the right hand side of Eq.(3) denotes the intensity of the object wave  $|O_d|^2$  and reference wave  $|R_d|^2$ . The last two terms represents the real image and the virtual one, respectively, where \* denotes the complex conjugation operation. The complex amplitude distribution of the object wave is obtained by the frequency spectrum filtering method and sequent angular spectrum reconstruction [21]:

$$O'(x_o, y_o) = \mathfrak{F}^{-1} \left\{ \mathfrak{F} \left[ \mathfrak{F}^{-1} \left\{ \text{filter} \left( \mathfrak{F}[H(x, y)] \right) \right\} \right] G_{-d}(f_x, f_y) \right\} \quad (4)$$

where the amplitude and phase distribution of objects is obtained as,

$$o'(x_o, y_o) = |O'(x_o, y_o)| \quad (5a)$$

$$\phi'(x_o, y_o) = \arctan \left\{ \frac{\text{Im}[O'(x_o, y_o)]}{\text{Re}[O'(x_o, y_o)]} \right\} \quad (5b)$$

We note that, in our simulations, after Frequency spectrum filtering method, the sparsity based compression technique is employed in order to reduce the dataset required for reconstruction. This operation, as noted above, eradicates most of the pixel values (set as zero) and small amount of pixels are considered in the hologram reconstruction process.

### 3. EXPERIMENTAL SETUP

The experimental set-up for continuous-wave (CW) terahertz off-axis digital holography is presented in Fig.1. A far-infrared radiation laser system pumped by a CO<sub>2</sub> laser (Edinburgh instrument Ltd.) is used to provide a 2.52 THz (wavelength is 118.83 mm) CW beam with output power of about 60 mW. The divergence angle of the output beam is about 13 milliarc-seconds and the diameter is about 11 mm. Two gold-coated off-axis parabolic mirrors were used to collimate and expand the beam. The off-axis hologram is recorded using a pyroelectric array detector (Pyrocam IV, Ophir- Spiricon), which has 320 × 320 pixels with a pixel size of 75 μm × 75 μm and pitch of 80 μm × 80 μm. The detector's frame rate is 48 Hz. We considered the sample of a metal coin with a diameter of about 14 mm is placed in front of the detector plane. The recording distance from the sample to the detector is 54 mm [24].

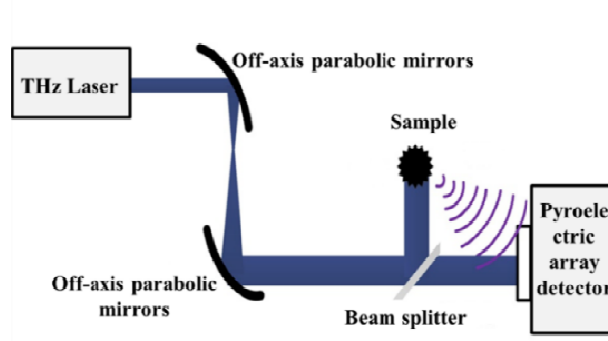


Fig.1. Experimental setup of continuous-wave terahertz based off-axis refractive digital holography.

We note that factors, for instance, low sensitivity of the pyroelectric detector and the air vibrations caused by enclosed camera chopper, affects the hologram recording [11]. As a consequent poor resolution (low peak signal to noise ratio) hologram was recorded. However, by repeating the capturing process, we captured 50 consecutive frames and image pre-processing is carried out in order to synthesize the high-quality holograms, for more details about image pre-processing see Ref [25]. It is mandatory that an appropriate propagation distance is estimated before reconstructing the focused sample distribution. In other words, the focused sample has clearly defined edge information [26]. Therefore, in order to estimate the edges, in our simulations, the Laplacian of Gaussian (LoG) filter is employed. It is known that the Laplacian (high-pass) filters are derivative filters that used to find the rapid change in image intensities. Since derivative filters are sensitive to noise information, therefore, it is common to smooth (low-pass) the image (e.g., Gaussian filter) before applying the Laplacian.

### 4. RESULTS

Experimental results are presented in this section. We used “One-Yuan Chinese” metal coin to record the hologram. Results of reconstruction (both amplitude and phase) are shown in Figure 2. In order to compare our results after sparse based reconstruction we used the standard Peak-signal to Noise Ratio (PSNR) as a performance metric [27]. The PSNR between both the original and sparse based reconstructed images are measured as,

$$\text{PSNR} = 10 \cdot \log_{10} \left( \frac{I_{\max}^2}{\text{MSE}} \right) \quad (6)$$

where  $I_{\max}$  is the maximum possible pixel value of the reconstructed images and MSE refers to the calculated mean squared error between the original and sparse based reconstructed images.

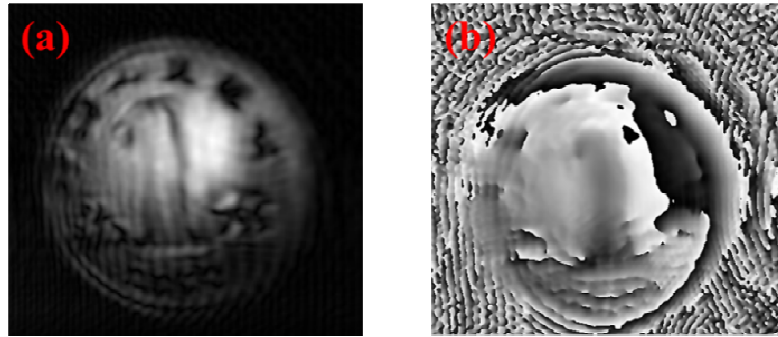


Fig.2. Reconstructed images: (a) amplitude image; (b) wrapped-phase image.

Figure 3 shows the sparsity based reconstructed images. It can be seen that information contained Furthermore, we have measured the PSNR values corresponding to the amount of applied sparsity to hologram.

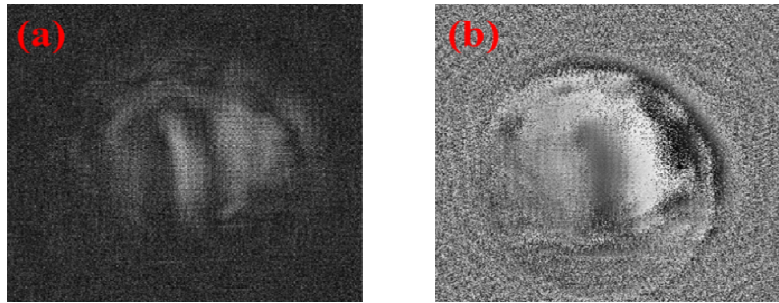


Fig.3. Sparse reconstructed images: (a) amplitude image; (b) wrapped-phase image.

Figure 4 depicts the graph plotted against amount of sparsity and PSNR values. From our simulations, it is estimated that 15% of original data is sufficient to reconstruct a hologram with decent image quality (PSNR = 25.16 dB).

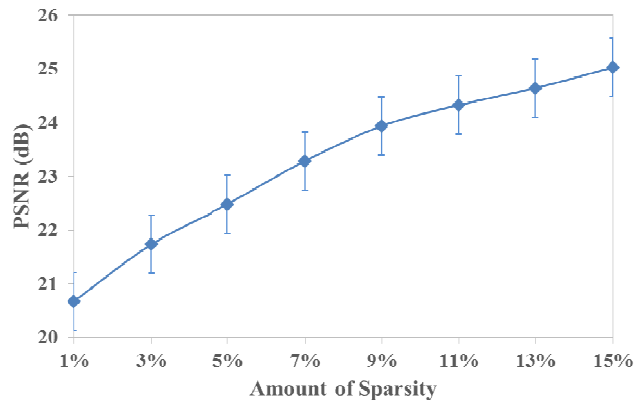


Fig.4. Amount of sparsity (%) vs PSNR (dB).

## 5. CONCLUSION

Terahertz radiation can be emitted over a wide spectral range and its radiation has a high penetration depth which makes it useful for security applications and non-destructive testing. In this paper, a continuous-wave Terahertz off-axis digital holographic system is described. It is known that hologram recording and reconstruction is computationally cumbersome for real-time object reconstruction or recognition, and is impractical for any type of holographic video streaming. Therefore, to alleviate, we have employed sparsity based hologram compression by which more efficient storage and transmission is facilitated.

## ACKNOWLEDGMENTS

Authors MW, LR and DW acknowledges the financial supports by the National Natural Science Foundation of China (61475011, 61307010), Science Foundation of Education Commission of Beijing (KZ201610005008), CAEP THz Science and Technology Foundation (201406), Young Talent Project of Beijing University of Technology, and the Special Matching Project of Local Supported by Centre. Graduate Science and Technology Fund of Beijing University of Technology (YKJ-2015-12539). IM acknowledges the support of Irish Research Council (IRC). RM is supported by the Iraqi Ministry of Higher Education and Scientific Research. JPR, JJH and JTS thanks Science Foundation Ireland (SFI), and Enterprise Ireland (EI) under the National Development Plan (NDP).

## REFERENCES

- [1] M. Perenzoni, and D. Paul, [Physics and Applications of Terahertz Radiation], Springer Netherlands Publisher, Netherlands, 173 (2014).
- [2] X. Xin, B. Ng, and D. Abbott, [Terahertz Imaging for Biomedical Applications: Pattern Recognition and Tomographic Reconstruction], Springer New York Publisher, New York, 978 (2012).
- [3] K. Peiponen, and J. A. Zeitler, [Terahertz Spectroscopy and Imaging], Springer-Verlag Berlin Heidelberg Publisher, Heidelberg, 171 (2013).
- [4] R. J. Mahon, J. A. Murphy, and W. Lanigan, "Digital holography at millimetre wavelengths", *Opt. Commun.* 260(2), 469-473 (2006).
- [5] M. S. Heimbeck, M. Kim, D. A. Gregory, and H. O. Everitt, "Terahertz digital holography using angular spectrum and dual wavelength reconstruction methods", *Opt. Express*, 19(10), 9192-9200 (2011).
- [6] S. Ding, Q. Li, Y. Li, and Q. Wang, "Continuous-wave terahertz digital holography by use of a pyroelectric array camera", *Opt. Lett.*, 36(11), 1993-1995 (2011).
- [7] M. Suga, Y. Sasaki, T. Sasahara, T. Yuasa, and C. Otani C, "THz phase-contrast computed tomography based on Mach-Zehnder interferometer using continuous wave source: proof of the concept", *Opt. Express*, 21(21), 25389-25402 (2013).
- [8] U. Schnars and W. Jüptner, "Direct recording of holograms by a CCD target and numerical reconstruction," *Appl. Opt.* 33, 179–181 (1994).
- [9] N. T. Shaked, J. Rosen, and A. Stern, "White-Light Single-Shot Digital Hologram Recorder," in *Adaptive Optics: Analysis and Methods/Computational Optical Sensing and Imaging/Information Photonics/Signal Recovery and Synthesis Topical Meetings on CD-ROM*, paper DTuD6 (2007).
- [10] D. Palima and J. Glückstad, "Comparison of generalized phase contrast and computer generated holography for laser image projection," *Opt. Express* 16, 5338-5349 (2008).
- [11] J. Rosen, "Three-dimensional holographic imaging," in *Frontiers in Optics*, OSA Technical Digest (CD), paper ThV2 (2003).
- [12] J. P. Ryle, D. S. Monaghan, S. McDonnell, and J. T. Sheridan, "Real world objects: capturing using in-line digital holography, projecting using spatial light modulators," *SPIE Optical Engineering+ Applications*, 74421B-74421B-7 (2009).
- [13] D. Gabor, "A new microscopic principle," *Nature* 161, 777–778 (1948).

- [14] T. J. Naughton, Y. Frauel, B. Javidi, and E. Tajahuerce, "Compression of digital holograms for three-dimensional object reconstruction and recognition," *Appl. Opt.* 41, 4124-4132 (2002).
- [15] Y. H. Seo, H. J. Choi, J. S. Yoo, G. S. Lee, C. H. Kim, S. H. Lee, S. H. Lee, and D. W. Kim, "Digital hologram compression technique by eliminating spatial correlations based on MCTF," *Opt. Commun.* 283(21), 4261-4270 (2010).
- [16] L. T. Bang, Z. Ali, P. D. Quang, J. H. Park, and N. Kim, "Compression of digital hologram for three-dimensional object using Wavelet-Bandelets transform," *Opt. Express* 19, 8019-8031 (2011).
- [17] D. J. Brady, K. Choi, D. L. Marks, R. Horisaki, and S. Lim, "Compressive Holography," *Opt. Express* 17, 13040-13049 (2009).
- [18] Y. Rivenson, A. Stern, and B. Javidi, "Overview of compressive sensing techniques applied in holography [Invited]," *Appl. Opt.* 52, A423-A432 (2013).
- [19] E. Le Pennec and S. Mallat, "Sparse geometric image representation with Bandelets," *IEEE Trans. Image Process.* 14(4), 423-438 (2005).
- [20] N. Demoli, H. Skenderović, and M. Stipčević, "Time-averaged photon-counting digital holography," *Opt. Lett.* 40, 4245-4248 (2015).
- [21] H. Huang, L. Rong, D. Wang, W. Li, Q. Deng, B. Li, Y. Wang, Z. Zhan, X. Wang, and W. Wu, "Synthetic aperture in terahertz in-line digital holography for resolution enhancement," *Appl. Opt.*, 55(3), A43-8 (2015).
- [22] J. W. Goodman, *Introduction to Fourier Optics*, Roberts and Company Publisher, New York, 3rd edition, (2005).
- [23] J. J. Healy, M. A. Kutay, H. M. Ozaktas, and J. T. Sheridan, [Linear Canonical Transforms: Theory and Applications], Springer Series in Optical Sciences 198 (2016).
- [24] M. Wan, D. Wang, L. Rong, Y. Wang, H. Huang, and B. Li, "Continuous-wave terahertz reflective off-axis digital holography," *Proc. SPIE 10157, Infrared Technology and Applications, and Robot Sensing and Advanced Control*, 101571U (2016).
- [25] L. Rong, T. Latychevskaia, D. Wang, X. Zhou, H. Huang, Z. Li, and Y. Wang, "Terahertz in-line digital holography of dragonfly hindwing: amplitude and phase reconstruction at enhanced resolution by extrapolation," *Opt. Express*, 22(14), 17236-17245 (2014).
- [26] H. Huang, D. Wang, L. Rong, X. Zhou, Z. Li, and Y. Wang, "Application of autofocusing methods in continuous-wave terahertz in-line digital holography," *Opt. Commun.*, 346, 93-98 (2015).
- [27] I. Muniraj, C. Guo, B. G. Lee, and J. T. Sheridan, "Interferometry based multispectral photon-limited 2D and 3D integral image encryption employing the Hartley transform," *Opt. Express* 23, 15907-15920 (2015).